SAND2011-3617C
Proceedings of Proceedings of the ASME 2011 International Mechanical Engineering Congress & Exposition
IMECE2011-64236
November 11-17, 2011, Denver, Colorado, USA

IMECE2011

A NONLOCAL APPROACH TO MODELING CRACK NUCLEATION IN AA 7075-T651

David J. Littlewood
Sandia National Laboratories
Multiscale Dynamic Materials Modeling (Org. 1435)
PO Box 5800, MS 1322
Albuquerque, NM 87185
Email: djlittl@sandia.gov

ABSTRACT

A critical stage in microstructurally small fatigue crack growth in AA 7075-T651 is the nucleation of cracks originating in constituent particles into the matrix material. Previous work has focused on a geometric approach to modeling microstructurally small fatigue crack growth in which damage metrics derived from an elastic-viscoplastic constitutive model are used to predict the nucleation event [1, 2]. While a geometric approach based on classical finite elements was successful in explicitly modeling the polycrystalline grain structure, singularities at the crack tip necessitated the use of a nonlocal sampling approach to remove mesh size dependence.

This study is an initial investigation of the peridynamic formulation of continuum mechanics as an alternative approach to modeling microstructurally small fatigue crack growth. Peridynamics, a nonlocal extension of continuum mechanics, is based on an integral formulation that remains valid in the presence of material discontinuities. To capture accurately the material response at the grain scale, an elastic-viscoplastic constitutive model is adapted for use in non-ordinary state-based peridynamics through the use of a regularized deformation gradient. The peridynamic approach is demonstrated on a baseline model consisting of a hard elastic inclusion in a single crystal. Coupling the elastic-viscoplastic material model with peridynamics successfully facilitates the modeling of plastic deformation and damage accumulation in the vicinity of the particle inclusion. Lattice orientation is shown to have a strong influence on material response.

INTRODUCTION

Microstructurally small fatigue crack (MSFC) growth comprises the majority of a component's life in the high-cycle fatigue regime [3]. To improve the accuracy of life estimation for the aluminum alloy AA 7075-T651, MSFC crack growth has been analyzed in terms of three phases: incubation, nucleation, and propagation [1]. For this material, fatigue cracks leading to component failure have been observed to form almost exclusively at particle inclusions. These inclusions provide incubation sites for fatigue cracks by way of pre-existing cracks that result from, for example, machining operations. The incubation phase consists of evolving grain-scale precursors to crack nucleation, for instance the formation of dislocation structures in the crystal lattice. The nucleation event is defined as the spawning of a matrix crack from a cracked particle inclusion into a surrounding grain. Nucleation is followed by microstructurally-small crack propagation, which may lead to the formation of a macro-scale fatigue crack and the eventual failure of a component.

A primary challenge in modeling MSFC growth in AA 7075-T651 is capturing the evolution of lattice-scale mechanisms in the direct vicinity of a pre-existing crack in a particle inclusion. Here, modeling efforts are forced to contend with singularities at the crack tip which typically preclude mesh convergence. The previous work of Hochhalter, *et. al*, addressed this problem through the use of a nonlocal sampling technique in which non-convergent metrics were sampled at a prescribed distance from the crack tip [2]. Peridynamics offers an alternative approach in which material discontinuities are handled naturally, removing

the need for auxilluary techniques.

The present study aims to apply peridynamics to the modeling of MSFC formation in AA 7075-T651. Peridynamics is a nonlocal extension of continuum mechanics that provides a mathematical description of material response that remains valid in the presence of discontinuities such as cracks. Two aspects of peridynamics are particularly well suited to modeling MSFC formation in AA 7075-T651: The ability to achieve mesh convergence in the vicinity of a crack, and the ability to model material failure through the breaking of peridynamic bonds. The current study is concerned primarily with the implementation of a (local) crystal plasticity material model within the (nonlocal) framework of peridynamics, and on a set of proof-of-concept simulations carried out using a simple baseline model. Coupling a crystal plasticity material model with peridynamics provides the groundwork for future studies on the application of damage metrics computed at the lattice scale as bond failure criteria.

PERIDYNAMICS METHODOLOGY

Peridynamics is a nonlocal extension of classical solid mechanics [4–6]. The peridynamic balance of linear momentum is formulated as an integral equation that remains valid in the presence of material discontinuities such as cracks. This is in contrast to classical continuum mechanics, in which the governing equations contain spatial derivatives that lead to singularities at material discontinuities.

The peridynamic model assumes direct nonlocal interaction between a point $\mathbf{x}$ and all points $\mathbf{x}'$ within the neighborhood of $\mathbf{x}$. The neighborhood of $\mathbf{x}$ is defined by a radius δ centered at $\mathbf{x}$, where δ is termed the horizon. The vector $\mathbf{x}'-\mathbf{x}$ is called a bond.

The peridynamic balance of linear momentum is

$$\rho(\mathbf{x})\ddot{\mathbf{u}}(\mathbf{x},t) = \mathbf{L}_{\mathbf{u}}(\mathbf{x},t) + \mathbf{b}(\mathbf{x},t) \qquad \forall\, \mathbf{x} \in \mathscr{B},\ t \geq 0, \tag{1}$$
$$\mathbf{L}_{\mathbf{u}}(\mathbf{x},t) = \int_{\mathscr{B}} \left\{ \underline{\mathbf{T}}[\mathbf{x},t]\left\langle \mathbf{x}'-\mathbf{x}\right\rangle - \underline{\mathbf{T}}'[\mathbf{x}',t]\left\langle \mathbf{x}-\mathbf{x}'\right\rangle \right\} \mathrm{d}V_{\mathbf{x}'}.$$

Here, $\mathscr{B}$ is the reference configuration of the body, ρ is the density in the reference configuration, $\mathbf{u}$ is the displacement, and $\mathbf{b}$ is the body force density.

The interaction between point $\mathbf{x}$ and a point $\mathbf{x}'$ in its neighborhood is governed by the force state at $\mathbf{x}$ at time t, denoted $\underline{\mathbf{T}}[\mathbf{x},t]$, and the force state at $\mathbf{x}'$ at time t, denoted $\underline{\mathbf{T}}'[\mathbf{x}',t]$. A force state is a function that associates with any bond $\mathbf{x}'-\mathbf{x}$ a force density per unit volume, $\underline{\mathbf{T}}[\mathbf{x},t]\left\langle \mathbf{x}'-\mathbf{x}\right\rangle$, acting on $\mathbf{x}$.

The numerical implementation of peridynamics employed in the current study is a meshless method in which the body $\mathscr{B}$ is discretized in the reference configuration into a finite number of spherical cells with each cell containing a single node at its center. The integral in Equation (1) is then be replaced by a summation,

$$\rho(\mathbf{x})\ddot{\mathbf{u}}_h(\mathbf{x},t) = \sum_{i=0}^{N} \left\{ \underline{\mathbf{T}}[\mathbf{x},t]\left\langle \mathbf{x}_i'-\mathbf{x}\right\rangle - \underline{\mathbf{T}}'[\mathbf{x}_i',t]\left\langle \mathbf{x}-\mathbf{x}_i'\right\rangle \right\} \Delta V_{\mathbf{x}_i'} + \mathbf{b}(\mathbf{x},t), \tag{2}$$

where N is the number of cells in the neighborhood of $\mathbf{x}$, $\mathbf{x}_i'$ is the position of the node centered in cell i, and $\Delta V_{\mathbf{x}_i'}$ is the volume of cell i.

Equation (2) requires evaluation of the force states $\underline{\mathbf{T}}[\mathbf{x},t]$ and $\underline{\mathbf{T}}'[\mathbf{x}_i',t]$. Force states are constitutive relationships that determine the pairwise force between a point $\mathbf{x}$ and each of its neighbors $\mathbf{x}_i'$. In general, the force state at $\mathbf{x}$ is a function of the deformations of all points within its neighborhoods and possibly other variables as well.

CRYSTAL ELASTIC-PLASTIC CONSTITUTIVE MODEL

In this study, constitutive behavior for AA 7075-T651 is captured with a crystal elastic-viscoplastic material model [1, 7, 8]. The material model, developed for use with classical finite element analysis, is adapted for peridynamics using the regularized deformation gradient scheme of Silling, *et. al* [5].

The constitutive model is based on a multiplicative decomposition of the deformation gradient [9],

$$\mathbf{F} = {}^{e}\mathbf{F}\,{}^{p}\mathbf{F}, \tag{3}$$

where ${}^{e}\mathbf{F}$ and ${}^{p}\mathbf{F}$ are the elastic and plastic deformation gradients, respectively. The elastic Green-Lagrange strain tensor is given by

$$ {}^{e}\hat{\mathbf{E}} = \frac{1}{2}\left({}^{e}\mathbf{F}^{T}\,{}^{e}\mathbf{F} - \mathbf{I}\right), \tag{4}$$

where ${}^{e}\mathbf{F}^{T}\,{}^{e}\mathbf{F}$ is the elastic Cauchy-Green deformation tensor, ${}^{e}\mathbf{C}$. Here, $\hat{}$ denotes the elastically unloaded configuration.

Behavior in the elastic regime is governed by a hyperelastic potential,

$$\hat{\mathrm{W}} = \hat{\mathrm{W}}({}^{e}\mathbf{F}) = \frac{1}{2}\,{}^{e}\mathbf{E} : \mathscr{L} : {}^{e}\mathbf{E}, \tag{5}$$

where $\mathscr{L}$ is the fourth-order elasticity tensor. The second Piola-Kirchhoff stress is given by

$$\hat{\mathbf{S}} = 2\frac{\partial \hat{W}}{\partial\, {}^{e}\mathbf{C}} = \mathscr{L} : {}^{e}\hat{\mathbf{E}}. \tag{6}$$

Elastic behavior is assumed anisotropic with cubic symmetry,

$$\mathscr{L}_{ijkn} = \mathscr{L}_{jikn} = \mathscr{L}_{ijnk} = \mathscr{L}_{knij}. \tag{7}$$

The Cauchy stress is found as the push-forward of the second Piola-Kirchhoff stress,

$$\sigma = {}^{e}\mathbf{F}\left(\frac{1}{\det({}^{e}\mathbf{F})}\mathbf{S}\right){}^{e}\mathbf{F}^{T}. \tag{8}$$

The plastic response is determined by crystallographic slip on each of the twelve slip systems in the face-centered cubic (FCC) lattice. The plastic velocity gradient, ${}^{p}\hat{\mathbf{L}}$, is given by

$${}^{p}\hat{\mathbf{L}} = \sum_{\alpha=1}^{12} \dot{\gamma}^{\alpha}\,\mathbf{P}^{\alpha}, \tag{9}$$

where $\dot{\gamma}^{\alpha}$ and $\mathbf{P}^{\alpha}$ are the rate of shearing and the Schmid tensor for slip system α, respectively. The Schmid tensor is given as

$$\mathbf{P}^{\alpha} = \mathbf{s}^{\alpha} \otimes \mathbf{m}^{\alpha}, \tag{10}$$

where $\mathbf{m}^{\alpha}$ and $\mathbf{s}^{\alpha}$ are the slip plane normal and the slip direction.

The slip rate on slip system α is related to the resolved shear stress on that slip system, τ^{α}, using a power law,

$$\dot{\gamma}^{\alpha} = \dot{\gamma}_{o}\frac{\tau^{\alpha}}{g^{\alpha}}\left|\frac{\tau^{\alpha}}{g^{\alpha}}\right|^{\frac{1}{m}-1}. \tag{11}$$

Here, $\dot{\gamma}_{o}$ is a reference slip rate, g^{α} is the hardness (resistance to slip) for slip system α, and m is a rate sensitivity parameter. The resolved shear stress on slip system α is found as

$$\tau^{\alpha} = \left({}^{e}\mathbf{C}\,\hat{\mathbf{S}}\right) : \mathbf{P}^{\alpha}. \tag{12}$$

The hardness values g^{α} evolve to capture hardening effects,

$$\dot{g}^{\alpha} = G_{o}\left(\frac{g_{s}-g^{\alpha}}{g_{s}-g_{o}}\right)\sum_{\beta} 2\left|\mathbf{P}^{\alpha}_{\text{sym}} : \mathbf{P}^{\beta}_{\text{sym}}\right|\left|\dot{\gamma}^{\beta}\right|, \tag{13}$$

where G_{o} is a hardening rate parameter, g_{o} is the initial hardness, g_{s} is the saturation hardness, and $\mathbf{P}_{\text{sym}}$ is the symmetric part of the Schmid tensor. The saturation hardness is given by

$$g_{s} = g_{so}\left|\frac{\dot{\gamma}}{\dot{\gamma}_{s}}\right|^{\omega}, \tag{14}$$

where ω is a material parameter, g_{so} is the initial saturation hardness, and $\dot{\gamma}$ is the total slip rate over all slip systems,

$$\dot{\gamma} = \sum_{\alpha=1}^{12}\left|\dot{\gamma}^{\alpha}\right|. \tag{15}$$

A series of damage metrics for the crystal plasticity constitutive model was investigated by Bozek, *et. al*, and Hochhalter, *et. al* [1, 2, 10]. Of these metrics, the Fatemi-Socie damage metric was selected for use in the current study [2, 11]. The Fatemi-Socie metric, as evaluated in the present study, is given by

$$D_{\text{Fatemi Socie}} = \max_{p}\int_{0}^{t}\sum_{\alpha=0}^{N_{d}}\left|\dot{\gamma}_{p}^{\alpha}\right|\left(1+k\frac{\left\langle\sigma_{n}^{p}\right\rangle}{g_{o}}\right)dt. \tag{16}$$

Here, $\max_{p}$ denotes the maximum value over the four slip planes, N_{d} is the number of slip systems per plane (three), and $\left\langle\sigma_{n}^{p}\right\rangle$ is the tensile stress on slip plane p. The parameter k dictates the relative importance of tensile stress relative to plastic slip and is set to 0.5 as suggested by Fatemi and Socie.

ADAPTION OF THE CRYSTAL ELASTIC-PLASTIC CONSTITUTIVE MODEL FOR USE WITH PERIDYNAMICS

The crystal plasticity material model described above was adapted for use with peridynamics using the method of non-ordinary state-base peridynamics developed by Silling, *et al.* [5]. The approach is based on an approximate (regularized) deformation gradient, $\bar{\mathbf{F}}$, evaluated at $\mathbf{x}$,

$$\bar{\mathbf{F}} = \left(\sum_{i=0}^{N}\underline{\omega}_{i}\,\underline{\mathbf{Y}}_{i}\otimes\underline{\mathbf{X}}_{i}\,\Delta V_{\mathbf{x}_{i}}\right)\mathbf{K}^{-1}, \tag{17}$$

where $\mathbf{K}$ is the shape tensor, defined as

$$\mathbf{K} = \sum_{i=0}^{N}\underline{\omega}_{i}\,\underline{\mathbf{X}}_{i}\otimes\underline{\mathbf{X}}_{i}\,\Delta V_{\mathbf{x}_{i}}. \tag{18}$$

Here, $\mathbf{X}_{i}$ denotes a vector directed from $\mathbf{x}$ to $\mathbf{x}'_{i}$ in the reference configuration, and, $\mathbf{Y}_{i}$ denotes a vector directed from $\mathbf{x}$ to $\mathbf{x}'_{i}$ in the deformed configuration. The operator $\otimes$ denotes dyadic product. The term $\underline{\omega}$ denotes an influence function that assigns a relative weighting to each neighbor $\mathbf{x}'_{i}$, for example based on the distance between $\mathbf{x}$ and $\mathbf{x}'$ in the reference configuration.

The approximate deformation gradient, as defined by Equation (17), provides the necessary kinematic input for a classical material model, *e.g.*, a material model developed for use with

classical finite element analysis. The stress state determined by the classical material model can then be transformed into peridynamic pairwise forces as follows,

$$\underline{\mathbf{T}}\left\langle \mathbf{x}' - \mathbf{x} \right\rangle = \underline{\omega}\mathbf{P}\mathbf{K}^{-1}\left\langle \mathbf{x}' - \mathbf{x} \right\rangle, \tag{19}$$

where $\mathbf{P}$ is the first Piola-Kirchhoff stress.

Equations (17) and (19) provide a means for applying the crystal plasticity constitutive model within the framework of peridynamics. Specifically, the approximate deformation gradient defined by Equation (17) is applied on the left-hand side of Equation (3). The Cauchy stress, found using Equation (8), is then converted to the first Piola-Kirchhoff stress by the relation

$$\mathbf{P} = \det\left({}^{e}\mathbf{F}\right)\boldsymbol{\sigma}\ {}^{e}\mathbf{F}^{-T}, \tag{20}$$

which allows for evaluation of the peridynamic pairwise forces using Equation (19).

SIMULATION OF A PARTICLE INCLUSION IN A SINGLE GRAIN

The peridynamic crystal plasticity model was evaluated through a set of simulations of a single crystal containing a single particle inclusion. The simulations were modeled after the 'baseline' simulations of Bozek, *et. al*, which were designed to be representative of conditions at the inner surface of a bolt hole where fatigue cracks have been observed to nucleate into the matrix material from cracked particle inclusions [1]. A representative volume containing a single crystal was constructed and 1% tensile strain applied in the horizontal direction (rolling direction), fixed boundary conditions applied in the vertical direction (normal direction), fixed boundary conditions applied on the back surface (tangential direction), and no boundary conditions applied on the front surface (*i.e.*, a free surface corresponding to the inner surface of the bolt hole). A single semi-hemispherical particle four microns in diameter was modeled on the free surface. The representative volume was constructed with an edge length equal to ten times the particle diameter in the vertical and horizontal directions, and five times the particle diameter in the direction normal to the free surface. The discretization of the model is shown in Figure 1.

Material properties for the aluminum alloy AA 7075-T651 were applied to the crystalline portion of the model, while the particle inclusion was modeled as linear elastic. The material properties for AA 7075-T651, given in Table 1, were derived by Bozek, *et. al*, using experimental data obtained by Jordan, *et. al* [1, 12]. For each simulation, one of two crystallographic orientations, denoted orientation A and orientation B, was assigned to the matrix material. Euler (Bunge) angles for the two crystal orientations are given in Table 2. The particle inclusion, modeled as isotropic linear elastic, was assigned a modulus of elasticity equal to 110% that of AA 7075-T651, and a Poisson's ratio and density equal to that of AA 7075-T651. Material properties for the particle inclusion are given in Table 3.

Simulations were carried out using the Sierra Mechanics analysis code at Sandia National Laboratories [13]. Time integration was implicit quasi-static, consisting of twenty equal load steps. Analyses were performed in parallel on eight CPU cores,

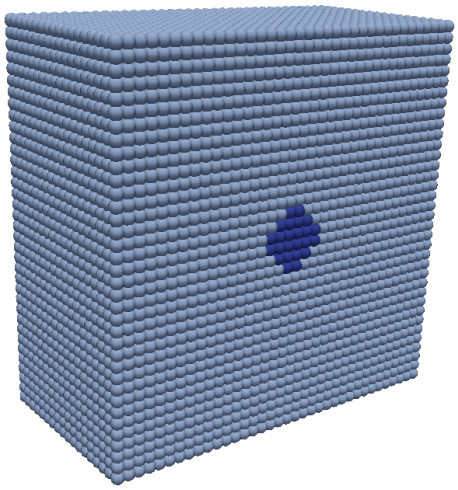

FIGURE 1. MODEL DISCRETIZATION

TABLE 1. MATERIAL PARAMETERS FOR AA 7075-T651

Parameter	Value
ρ	2.81e-9 tonne/mm^3
λ	60.9e3 MPa
μ	28.3e3 MPa
η	5.1e3 MPa
m	0.005
g_o	220.0 MPa
$\dot{\gamma}_o$	1.0 s^{-1}
G_0	120.0 MPa
g_{s_o}	250.0 MPa
$\dot{\gamma}_s$	5.0e10 s^{-1}
ω	0.0

TABLE 2. LATTICE ORIENTATIONS (RADIANS)

	Euler Angles (ϕ_1, Φ, ϕ_2)
Orientation A	(0.9738, 0.4322, -1.3822)
Orientation B	(1.9490, 0.8644, -2.120)

TABLE 3. MATERIAL PARAMETERS FOR HARD INCLUSION

Parameter	Value
ρ	2.81e-9 tonne/mm^3
λ	66.99e3 MPa
μ	31.13e3 MPa
η	0.0 MPa

with run times of approximately one hour.

The influence of crystallographic orientation was evaluated under several conditions. For each of the lattic orientations listed in Table 2, a simulation was carried out using an intact particle, followed by a simulation in which the particle contained a pre-crack normal to the loading direction, as described in the following section.

RESULTS

Result are presented below for the case of an uncracked particle inclusion and of a cracked particle inclusion. In both cases, simulations were carried out using two different lattice orientations to investigate the influence of grain orientation on material response.

For the purpose of visualizing material response in the vicinity of the particle inclusion, Figures 2–6 include images corresponding to a cubic section of the model approximately ten microns in each dimension. Here, the front face corresponds to the free surface and is centered around the particle inclusion. The inclusion itself was ommitted from these illustrations to allow for visualization of the subsurface material response.

Uncracked Particle Inclusion

Material response for the uncracked particle simulations is presented in Figures 2, 3, and 4. Plots of the average stress in the particle inclusion and of the total crystallographic slip over the representative volume are presented in Figure 2. Orientation B was found to be more favorable for crystallographic slip under the prescribed loading conditions. As a result, the final average

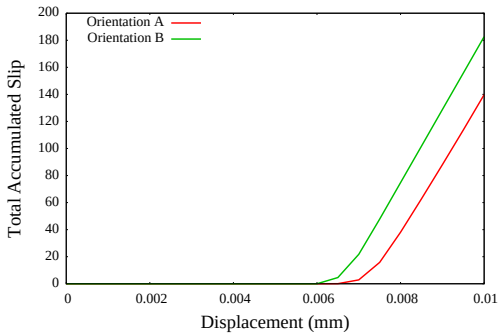

(a) Total crystallographic slip.

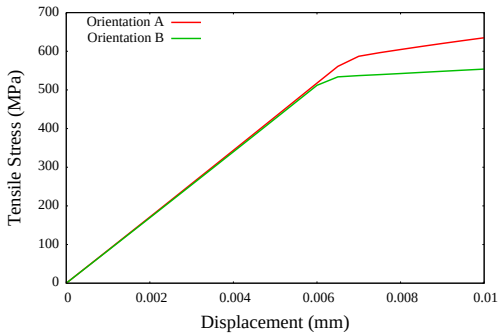

(b) Average particle stress.

FIGURE 2. MATERIAL RESPONSE FOR THE UNCRACKED PARTICLE SIMULATIONS

stress in the particle inclusion was higher for orientation A.

Plastic flow on each of the twelve available slip systems over the course of the simulation is presented in Figures 3(a) and 4(a). Orientation A shows a single dominate slip system, while a pair of dominate slip systems is active for orientation B. As illustrated in Figures 3 and 4, orientation A contains a pronounced plane of plastic flow in the vicinity of the particle inclusion, while orientation B displays a highly symmetric pattern of plastic flow. A high concentration of deformation is observed at the top and bottom of the inclusion for orientation B.

Cracked Particle Inclusion

Material response for the simulations containing a cracked particle inclusion are presented in Figures 5 and 6. As expected, the presence of a crack through the diameter of the particle inclusion has a pronounced effect on system response. Deformation is now concentrated at the top and bottom of the particle inclusion for both orientation A and B. Due to their direct proximity to the crack tip, these areas undergo significant plastic deformation and are possible sites for crack nucleation from the cracked particle into the neighboring grain.

The Fatemi-Socie damage metric, defined in Equation (16), is illustrated in Figures 5(c) and 6(c). The Fatemi-Socie metric

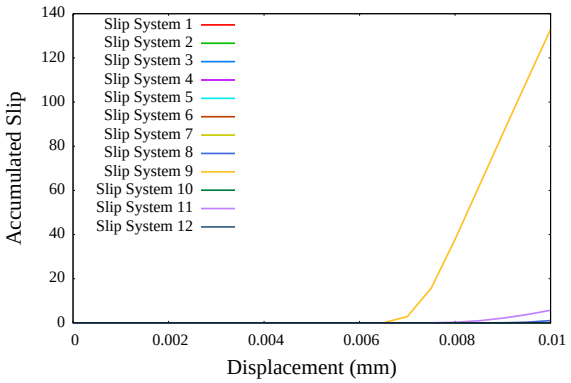

(a) Behavior on individual slip systems for orientation A.

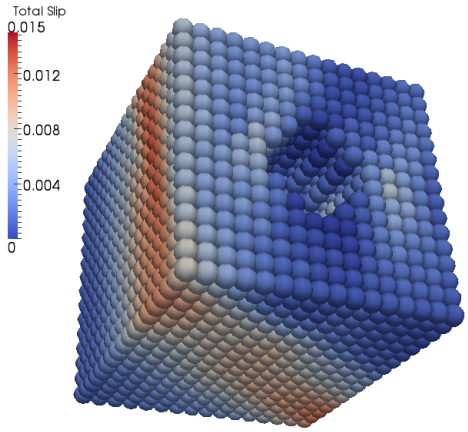

(b) Total slip over all slip systems for orientation A.

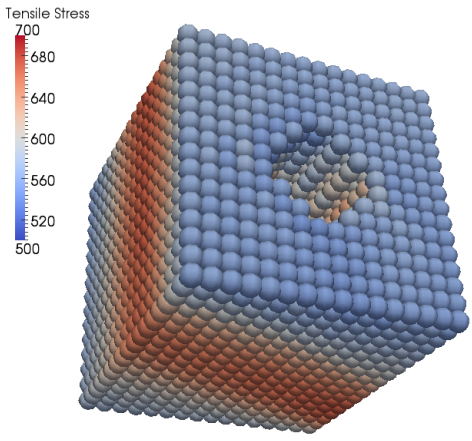

(c) Tensile stress for orientation A.

FIGURE 3. MATERIAL RESPONSE IN THE VICINITY OF AN UNCRACKED PARTICLE, ORIENTATION A.

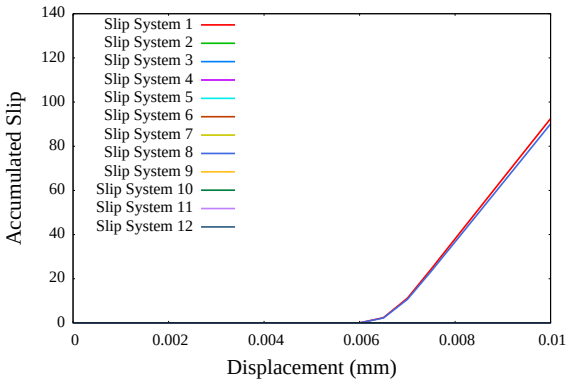

(a) Behavior on individual slip systems for orientation B.

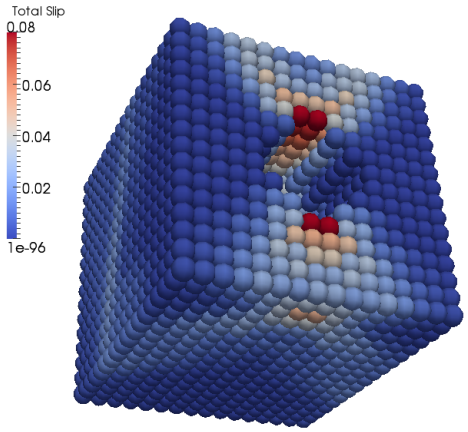

(b) Total slip over all slip systems for orientation B.

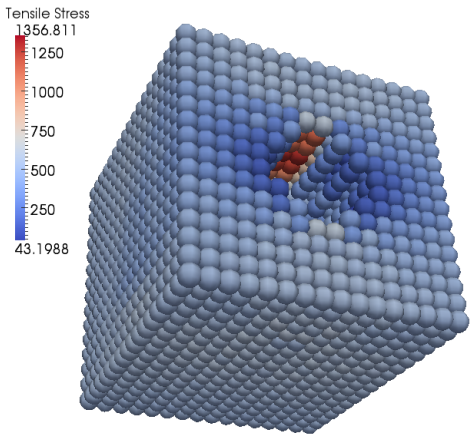

(c) Tensile stress for orientation B.

FIGURE 4. MATERIAL RESPONSE IN THE VICINITY OF AN UNCRACKED PARTICLE, ORIENTATION B.

is a function of both stress and plastic deformation in the vicinity of the crack tip, reflecting the idea that plastic deformation (*e.g.* dislocation entanglement) is a precursor to crack nucleation that is triggered by the stress state. The results suggest that crack nucleation into the matrix material may be more likely in the case of orientaiton B than in the case of orientation A.

DISCUSSION AND CONCLUSIONS

In this study, a crystal elasto-viscoplastic material model was adapted for use within the peridynamic framework for nonlocal mechanics. This was motivated by the need to model accurately the deformation state in the vicinity of cracked particle inclusions in AA 7075-T651. The crystal plasticity material model was coupled to peridynamics by way of an approximate deformation gradient. This approach was validated through the simulation of tensile loading applied to a single crystal containing a single particle inclusion. The lattice orientation of the crystal was found to have a strong influence on the material response, including the stress state, plastic deformation, and material damage as modeled by a Fatemi-Socie metric.

Current Work

The present study provides a foundation for ongoing work in nonlocal crystal plasticity. Current areas of research include mesh-independent modeling of plastic zones in the vicinity of a crack tip, the modeling of crack nucleation and subsequent crack propagation into the matrix material, and peridynamic simulations of realistic polycrystal models. Also underway is the study of zero-energy model supression for non-ordinary state-based peridynamics, and the performance of non-ordinary state-based peridynamics on nonuniform discretizations.

SANDIA NATIONAL LABORATORY

Sandia National Laboratories is a multi-program laboratory managed and operated by Sandia Corporation, a wholly owned subsidiary of Lockheed Martin Corporation, for the U.S. Department of Energy's National Nuclear Security Administration under contract DE-AC04-94AL85000.

ACKNOWLEDGMENT

The author would like to acknowledge the large number of people who have supported this study. The crystal plasticity material model was developed under the direction of Antoinette Maniatty in collaboration with Jacob Hochhalter, Michael Veilleux, Jeff Bozek, Paul Wawrzynek, and Anthony Ingraffea. The author would like to acknowledge Stewart Silling for the original formulation of peridynamics, as well as John Foster, Richard Lehoucq, John Mitchell, and Michael Parks for their contributions in support of this project. The author would also like to acknowledge

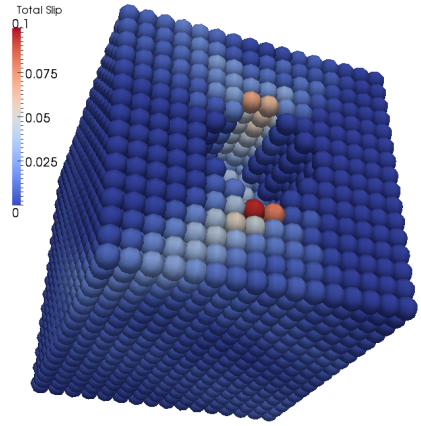

(a) Total slip over all slip systems for orientation A.

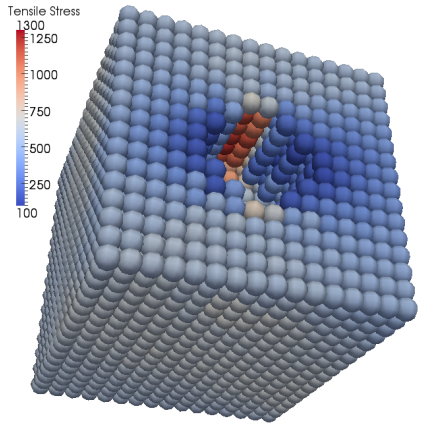

(b) Tensile stress for orientation A.

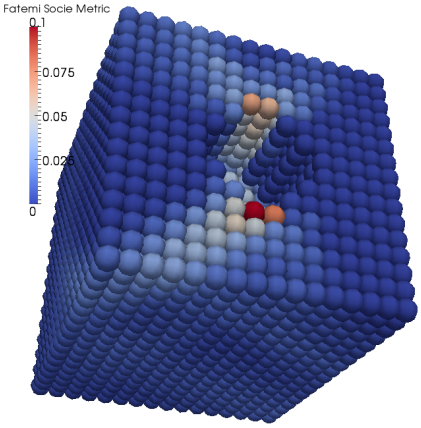

(c) Fatemi-Socie damage metric for orientation A.

FIGURE 5. MATERIAL RESPONSE IN THE VICINITY OF A CRACKED PARTICLE, ORIENTATION A.

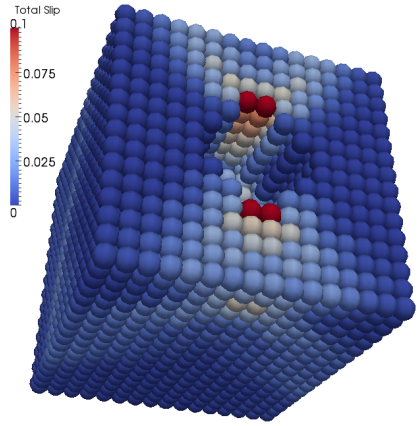

(a) Total slip over all slip systems for orientation B.

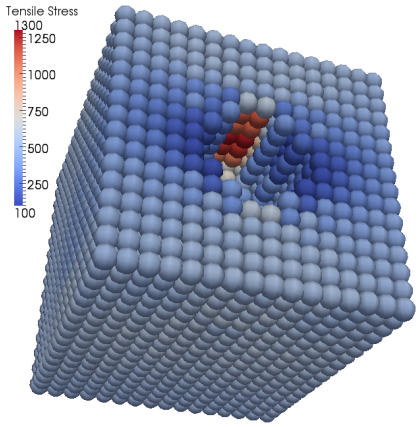

(b) Tensile stress for orientation B.

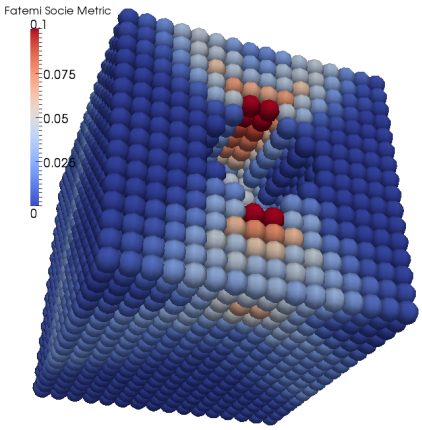

(c) Fatemi-Socie damage metric for orientation B.

FIGURE 6. MATERIAL RESPONSE IN VICINITY OF CRACKED PARTICLE, ORIENTATION B.

the Sierra Mechanics development team: Nathan Crane, Martin Heinstein, Alex Lindblad, Kyran Mish, Kendall Pierson, Vicki Porter, Nathaniel Roehrig, Timothy Shelton, Gregory Sjaardema, Benjamin Spencer, and Jesse Thomas.

REFERENCES

[1] Bozek, J. E., Hochhalter, J. D., Veilleux, M. G., Liu, M., Heber, G., Sintay, S. D., Rollett, A. D., Littlewood, D. J., Maniatty, A. M., Weiland, H., Christ, Jr., R. J., Payne, J., Welsh, G., Harlow, D. G., Wawrzynek, P. A., and Ingraffea, A. R., 2008. "A geometric approach to modeling microstructurally small fatigue crack formation: I. Probabilistic simulation of constituent particle cracking in AA 7075-T651". *Modelling and Simulation in Materials Science and Engineering,* ***16***(6).

[2] Hochhalter, J. D., Littlewood, D. J., Christ, Jr., R. J., Veilleux, M. G., Bozek, J. E., Ingraffea, A. R., and Maniatty, A. M., 2010. "A geometric approach to modeling microstructurally small fatigue crack formation: II. Physically based modeling of microstructure-dependent slip localization and actuation of the crack nucleation mechanism in AA 7075-T651". *Modelling and Simulation in Materials Science and Engineering,* ***18***(4).

[3] Suresh, S., 1998. *Fatigue of materials*, 2nd ed. Cambridge University Press, Cambridge, MA.

[4] Silling, S., 2000. "Reformulation of elasticity theory for discontinuities and long-range forces". *Journal of the Mechanics and Physics of Solids,* ***48***(1), pp. 175–209.

[5] Silling, S., Epton, M., Weckner, O., Xu, J., and Askari, E., 2007. "Peridynamic states and constitutive modeling". *Journal of Elasticity,* ***88***(2), pp. 151–184.

[6] Silling, S. A., and Lehoucq, R. B., 2010. "Peridynamic theory of solid mechanics". *Advances in Applied Mechanics,* ***44***, pp. 73–168.

[7] Matouš, K., and Maniatty, A., 2004. "Finite element formulation for modeling large deformations in elasto-viscoplastic polycrystals". *International Journal for Numerical Methods in Engineering,* ***60***, pp. 2313–2333.

[8] Pyle, D., 2009. "A comparison of 2 methods for FEM simulations of discretized polycrystals". PhD thesis, Rensselaer Polytechnic Institute, Troy, New York.

[9] Lee, E., 1969. "Elastic-plastic deformation at finite strain". *Journal of Applied Mechanics,* ***36***, pp. 1–6.

[10] Hochhalter, J. D., Littlewood, D. J., Veilleux, M. G., Bozek, J. E., Maniatty, A. M., Rollett, A. D., and Ingraffea, A. R., 2011. "A geometric approach to modeling microstructurally small fatigue crack formation: III. Development of a semi-empirical model for nucleation". *Modelling and Simulation in Materials Science and Engineering,* ***19***(3).

[11] Fatemi, A., and Socie, D. F., 1988. "A critical plane approach to multiaxial fatigue damage including out-of-phase

loading". *Fatigue and Fracture of Engineering Materials and Structures,* ***11***(3), pp. 149–65.

[12] Jordan, J. B., Horstemeyer, M. F., Solanki, K., and Xue, Y., 2007. "Damage and stress state influence on the bauschinger effect in aluminum alloys". *Mechanics of Materials,* ***39***(10), pp. 920–931.

[13] Edwards, C. H., and Stewart, J. R., 2001. "SIERRA: A software environment for developing complex multiphysics applications". In First MIT Conference on Computational Fluid and Solid Mechanics, K. Bathe, ed., pp. 1147–1150.